Kinematics and U-Pb dating of detrital zircons from the Sierra de Zacatecas, Mexico

Felipe de Jesús Escalona-Alcázar[1,2,3,*], Luis Alberto Delgado-Argote[2], Bodo Weber[2], Ernesto Patricio Núñez-Peña[4], Víctor A. Valencia[5], and Olivia Ortiz-Acevedo[1]

[1] *Departamento de Ordenamiento Ecológico, Instituto de Ecología y Medio Ambiente de Zacatecas,*
Av. México 151, Col. La Florida, 98600 Guadalupe, Zacatecas, Mexico.
[2] *División de Ciencias de la Tierra, Centro de Investigación Científica y de Educación Superior de Ensenada (CICESE),*
Km. 107 Carr. Tijuana-Ensenada, 22860, Ensenada, Baja California, Mexico.
[3] *Faculty of Earth and Life Sciences, Vrije Universiteit Amsterdam,*
De Boelelaan 1085, 1081 HV Amsterdam, The Netherlands.
[4] *Unidad de Ciencias de la Tierra, Universidad Autónoma de Zacatecas,*
Calzada de la Universidad 108, Col. Progreso, 98058, Zacatecas, Zacatecas, Mexico.
[5] *Department of Geosciences, University of Arizona,*
1040 East Fourth St., Tucson, AZ, 85721-0077, United States of America.
*escalona@cicese.mx

ABSTRACT

The Mesozoic succession of the Sierra de Zacatecas (SZ) was originally described in two sequences. The older is the La Pimienta Phyllite or sometimes termed Zacatecas Formation (ZF) of presumably Late Triassic age based on paleontological constraints obtained at the beginning of the twentieth Century. Overlying the ZF is Las Pilas Volcanosedimentary Complex (LPVC) of unknown age, whose contact has been interpreted to be tectonic. We have studied these sequences in detail in order to constrain their stratigraphic relationships, deformation style, composition, and maximum depositional age.

The ZF has been metamorphosed under greenschist facies conditions and its protolith is composed of sandstone, mudstone, limestone and rare conglomerates interlayered with lava flows and tuffs. This unit is intruded by dikes, sills, laccolithic bodies and we interpret the presence of hydrothermal vents at the type locality in the Arroyo El Bote. The ZF is in our interpretation in gradual contact with the LPVC. The LPVC is an igneous assemblage mainly made up of mafic pillowed to massive flows, commonly foliated and/or deformed. Contemporaneous laccolithic-like bodies, dikes and sills are observed. Feldespatic greywackes and wackes, mudstone and minor tuffs and limestone are interbedded within the lava flows. U-Pb dating of detrital zircons from ZF and LPVC from the Arroyo El Bote and the Sauceda de la Borda areas, respectively, yielded ~132 Ma and ~160 Ma old ages. Approximately 30% of the zircons from the ZF represent Paleozoic and Proterozoic inheritance, which is lacking in the LPVC, and suggests a change in the sedimentary source. The maximum depositional age for both sequences in this area is therefore interpreted as Early Cretaceous (Hauterivian), in contrast to the previous proposed Late Triassic age. According to the distribution and types of rocks, the volcano-plutonic and sedimentary assemblage may have been emplaced in a volcanic field that developed in an intra-arc or back-arc basin with sedimentary supply derived from a nearby continental block and a magmatic arc.

The geometric analysis of foliation shows that the average poles of the ZF and LPVC are 86º/235º and 86º/244º, respectively. The paleostress analysis yield an average σ1 for the thrust faults at 01º/219º suggesting that foliation and reverse faulting should have been developed contemporaneously during the Laramide Orogeny. Normal faults formed during a later extensional regime are associated to an average σ3 vector oriented 00º/029º. Since normal faults always cut the thrust faults, we interpret that normal faults developed in a post-orogenic event.

Key words: stratigraphy, detrital zircon geochronology, paleostress, Hauterivian, Zacatecas, Mexico.

RESUMEN

Desde las primeras descripciones, las rocas mesozoicas de la Sierra de Zacatecas se han descrito en dos secuencias. La más antigua corresponde a la Filita La Pimienta o Fm. Zacatecas (ZF), cuya edad paleontológica es del Triásico Tardío. También se ha descrito que está en contacto tectónico con el Complejo Volcanosedimentario Las Pilas (LPVC), cuya edad se desconoce. En este trabajo se estudiaron con detalle las composiciones, relaciones de contacto, estilos de deformación y edades de depósito de dichas secuencias litológicas en la parte central y norte de la Sierra de Zacatecas.

La ZF presenta metamorfismo en facies de esquistos verdes y está compuesta por areniscas, lodolitas, calizas y, en menor medida, conglomerados interestratificados con derrames lávicos y tobas. La secuencia está intrudida por diques, sills, lacolitos dioríticos, e interpretamos la presencia de ventilas hidrotermales en la localidad tipo. El contacto con la LPVC es gradual. El LPVC está formado por series de lavas máficas cuyas texturas varían de almohadilladas a masivas, comúnmente foliadas y deformadas. La secuencia volcánica puede estar interestratificada con wacka, grauvaca, lodolita y, en menor cantidad, tobas y caliza. También hay cuerpos lacolíticos, diques y sills asociados a las rocas volcánicas. Las edades isotópicas U-Pb de zircones detríticos de la ZF y LPVC de una muestra obtenida en el Arroyo El Bote y otra en el área de Sauceda de la Borda, respectivamente, inidcan que provienen de una fuente cuya edad es de ~132 Ma y ~160 Ma. Aproximadamente 30% de los granos analizados de la ZF tienen edades más antiguas, del Paleozoico al Arqueano. En cambio en la muestra de la LPVC los zircones más antiguos son del Jurásico Tardío. La edad máxima de depósito de ambas secuencias se define como del Cretácico Temprano (Hauteviriano), en contraste con la edad del Triásico Tardío asignada en trabajos anteriores. De acuerdo con la distribución y tipos de roca, la asociación volcano-plutónica y sedimentaria definiría un campo volcánico que pudo desarrollarse en un ambiente interior de arco o de trasarco, con sedimentos provenientes de un bloque continental y de un arco magmático.

Del análisis geométrico de la foliación de la ZF y del LPVC, se observa que las orientaciones promedio de sus polos son 86º/235º y 86º/244º, respectivamente. A partir del análisis de paleoesfuerzos se obtuvo un promedio de σ1 para fallas inversas de 01º/219º, lo que sugiere que la foliación y el fallamiento inverso pudieron haberse desarrollado de forma contemporánea durante la Orogenia Laramide. El fallamiento normal se desarrolló posteriormente en un régimen extensional con una orientación promedio del vector σ3 de 00º/029º. Debido a que las fallas normales cortan a las inversas, interpretamos que el fallamiento normal se desarrolló en un evento post-orogénico.

Palabras clave: estratigrafía, geocronología de zircones detríticos, paleoesfuerzos, Hauteriviano, Zacatecas, México.

INTRODUCTION

The Sierra de Zacatecas (SZ) is a topographic high located in the central part of the State of Zacatecas (Figure 1a). This is one of the few outcrops north of the Trans-Mexican Volcanic Belt (TMVB) with a Mesozoic igneous and clastic sedimentary rock assemblage (Figure 1a). The origin and tectonic setting of the Mesozoic sequence of the SZ are controversial. However there is a general agreement in relating it to the Guerrero terrane (GT) (Centeno-García and Silva-Romo, 1997) or Guerrero Superterrane (Dickinson and Lawton, 2001) (Figure 1a). The GT is made up of an island arc, back-arc and ocean-floor assembly of Triassic to Early Cretaceous age (Centeno-García and Silva-Romo, 1997). Although the terrane has been extensively studied south of the TMVB, the limited outcrops in the northern areas make it difficult to delineate its northeastern boundaries. The closest locations to SZ where the Guerrero terrane has been analyzed are Guanajuato (Tardy and Maury, 1973; Lapierre *et al*., 1992; Ortiz-Hernández *et al*., 1992, 2003; Tardy *et*

al., 1992, 1994; Freydier *et al*., 1996, 1997, 2000), the Baja California peninsula (Dickinson and Lawton, 2001; Busby *et al*., 2006), State of Mexico (Delgado-Argote *et al*., 1992), Guerrero (Delgado-Argote *et al*., 1992; Talavera-Mendoza *et al*., 2007) and Sinaloa (Ortega-Gutiérrez *et al*., 1979, Gastil *et al*., 1999) (Figure 1a). Under this scenario, the age and tectonic setting of the SZ is of great significance in defining the probable extension of the GT, and will improve the knowledge on the geologic evolution of central Mexico during the Mesozoic.

The Sierra de Zacatecas is located in the central part of Mexico (Figure 1a). It is subdivided in two major stratigraphic units (Burckhardt, 1906; Gutiérrez-Amador, 1908; McGehee, 1976; Ranson *et al*., 1982; Sedlock *et al*., 1993; Centeno-García and Silva-Romo, 1997; Barboza-Gudino *et al*., 1999; Silva-Romo *et al*., 2000; Bartolini *et al*., 2001).

The lowermost stratigraphic unit is the Zacatecas Fm. (ZF) (Gutiérrez-Amador, 1908), sometimes also called La Pimienta Phyllite (Ranson *et al*., 1982), which crops out in the western part of the SZ. The ZF is overlain by a litho-
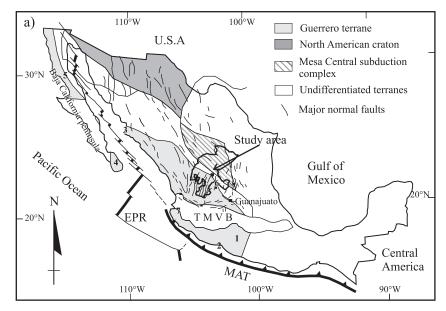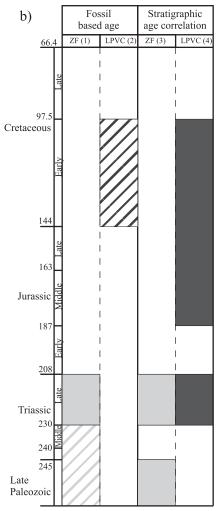
Figure 1. a: Cartoon showing the location of the study area together with the main tectonic boundaries and normal faults of central and western Mexico (modified from Dickinson and Lawton, 2001). Abbreviations: TMVB: Trans Mexican Volcanic Belt, EPR: East Pacific Rise, and MAT: Middle America Trench. Bold line is the boundary of the State of Zacatecas. Bold numbers are the approximate locations of some ages from the Guerrero terrane. 1: San Pedro Limón, 104±6 to 114±3 Ma, ^{40}Ar/^{39}Ar plateau age in hornblende (Delgado-Argote *et al.*, 1992); 2: Loma Baya-El Tamarindo, 112±3 Ma, ^{40}Ar/^{39}Ar plateau age in hornblende (Delgado-Argote *et al.*, 1992); 3: Porohui, 86.3±2.4 Ma, ^{40}Ar/^{39}Ar plateau age in whole rock (Gastil *et al.*, 1999); 4: La Paz-Todos los Santos, 116±6 Ma, K-Ar in hornblende, cooling age (Murillo-Muñetón, 1991 *in* Sedlock *et al.*, 1993); 5: Arroyo Calamajué, ~122 Ma, U-Pb in zircon (Gastil *et al.*, 1991 *in* Sedlock *et al.*, 1993); 6: San Nicolas, 147.9 to 151.3 Ma in zircons (Mortensen *et al.*, 2008); and 7: The Cuale River Mining Disctrict, 154.0 to 157.2 Ma in zircons (Bissig *et al.*, 2008). b: Table showing the ages proposed by several authors for the ZF (light gray) and LPVC (dark gray). Stippled patterns are for uncertain ages reported in the literature. References as follow 1: Burckhardt (1906); 2: Yta (1993) personal communication *in* Centeno-García and Silva-Romo (1997); 3: Yta *et al.* (2003), Silva-Romo *et al.* (2000); 4: Centeno-García and Silva-Romo (1997); Silva-Romo *et al.* (2000). The period and epoch boundaries are in Ma (Palmer, 1983).

logic unit that has received several names: the Zacatecas greenstone (McGehee, 1976), Las Pilas Diorite (Ranson *et al.*, 1982), Zacatecas Microdiorite (Ponce and Clark, 1988) or La Borda Fm. (Centeno-García and Silva-Romo, 1997). As named and described by Ransom *et al.* (1982), Las Pilas Volcanosedimentary Complex (LPVC) is the name given to the lithologic unit above ZF. The ZF and the LPVC are supposed to have formed, developed and evolved in different tectonic settings prior to their amalgamation to the North America craton during the Late Cretaceous (Centeno-García *et al.*, 1993; Busby *et al.*, 2006) or the Late Cretaceous – Early Tertiary (Aranda-Gómez *et al.* 2000) Laramide Orogeny.

Some of the key questions arising from the revision of the literature and our geologic survey are: 1) Are the ZF and the LPVC two different facies of a single volcanosedimentary complex?; 2) What are their depositional ages?; 3) In what kind of tectonic environments the ZF was juxtaposed with the LPVC?. To address these issues we conducted a detailed geologic survey to define and describe the stratigraphy and the contact relationships of the ZF and LPVC in the

SZ. In order to establish a maximum age of the sequences, we separated detrital zircons for LA-ICPMS dating from one sample of the ZF and one from the LPVC. Based on these results, we propose a new interpretation on the origin and evolution of the Sierra de Zacatecas.

PREVIOUS STRATIGRAPHY AND AGE CONSTRAINTS

The lithologic compositions of the ZF and the LPVC are controversial. The ZF has been described as a mainly detrital sedimentary package associated with coeval volcanic rocks (Burckhardt, 1906; Gutiérrez-Amador, 1908; McGehee, 1976; Ranson *et al.*, 1982; Monod and Calvet, 1992; Sedlock *et al.*, 1993; Centeno-García and Silva-Romo, 1997; Yta *et al.*, 2003) or without them (Barboza-Gudino *et al.*, 1999; Silva-Romo *et al.*, 2000; Bartolini *et al.*, 2001). The ZF has been interpreted as a flysch-like deposit that formed a submarine fan close to the western passive margin of Pangea (Monod and Calvet, 1992; Barboza-Gudino *et al.*,

(1999); Silva-Romo *et al.*, 2000; Bartolini *et al.*, 2001). In contrast Gutiérrez-Amador (1908) and Monod and Calvet (1992) suggested a shallow marine environment.

The first study that interpreted an Upper Triassic age for the ZF, based on fossil evidence, was made by Burckhardt (1906). Such interpretation has been widely adopted or even re-interpreted as Middle to Upper Triassic age (Figure 1b) (Gutiérrez-Amador, 1908; McGehee, 1976; Ranson *et al.*, 1982; Sedlock *et al.*, 1993; Barboza-Gudino *et al.*, 1999; Silva-Romo *et al.*, 2000; Bartolini *et al.*, 2001). Silva-Romo *et al.* (2000) considered the upper part of the ZF as Middle Jurassic. Yta *et al.* (2003) further considered the possibility of a late Paleozoic age, as was originally suggested by Burckhardt (1906). Reported ages for the LPVC, based on stratigraphic correlation, are also controversial and vary from Early Cretaceous (Monod and Calvet, 1992; Centeno-García and Silva-Romo, 1997; Yta *et al.*, 2003) to Late Jurassic (Sedlock *et al.*, 1993) (Figure 1b). On the basis of geochemical data, the tectonic setting for the ZF has been interpreted as an ocean-basin or primitive island arc (Centeno-García y Silva-Romo 1997), while for the LPVC is interpreted as an oceanic island arc (Lapierre *et al.*, 1992).

The LPVC has been barely studied and its stratigraphic relationships with the ZF have been interpreted in several ways. The contact has been described to be tectonic (Monod and Calvet, 1992; Centeno-García and Silva-Romo, 1997; Silva-Romo *et al.*, 2000; Bartolini *et al.*, 2001), discordant (McGehee, 1976), obscure (Sedlock *et al.*, 1993) or continuous (Burckhardt, 1906; Gutiérrez-Amador, 1908; McGehee, 1976; Ranson *et al.*, 1982).

The LPVC has been described as a laccolith-like or hypabyssal intrusion of andesitic composition (McGehee, 1976; Ranson *et al.*, 1982). Some igneous rocks were generically described as intrusive and other as extrusive (Ranson *et al.*, 1982), or as pillows and massive basaltic to andesitic lava flows interlayered with volcanoclastics, limolite and radiolarite (Lapierre *et al.*, 1992; Centeno García and Silva-Romo, 1997; Yta *et al.*, 2003). According to Centeno-García and Silva-Romo (1997), and Mortensen *et al.* (2008), the depositional facies of the LPVC could correspond to a deep water marine environment that developed in an intra-arc basin or back-arc basin.

Tectonic evolution

The ZF has experienced greenschist facies metamorphism and ductile deformation that promoted the formation of a foliation that varies in intensity from moderately to well developed, sometimes exhibiting crenulation cleavage, locally tightly folded. The style of deformation, age and duration have been poorly studied. Research works by McGehee (1976) and Ranson *et al.* (1982) indicate at least two deformation stages for the ZF. However, because of the limited amount of data, these results are inconclusive.

Most authors agree that at least two deformation phases are responsible for the deformation of the Mesozoic sequence of the SZ: the first one is pre-Early Cretaceous age and the second one is Late Cretaceous-early Tertiary (Monod and Calvet, 1992; Sedlock *et al.*, 1993; Centeno-García and Silva-Romo, 1997; Goldhammer, 1999; Silva-Romo *et al.*, 2000; Dickinson and Lawton, 2001; Yta *et al.*, 2003). In addition, Bartolini *et al.* (2001) also suggested a third deformation phase that occurred during the Late Triassic-Early Jurassic (?) time.

By correlation, the origin and evolution of the LPVC has been interpreted to belong to the Guerrero terrane of Late Jurassic-Early Cretaceous age of southern and central Mexico (De Cserna, 1976; Campa and Coney, 1983; Sedlock *et al.*, 1993; Centeno-García and Silva-Romo, 1997; Silva-Romo *et al.*, 2000; Dickinson and Lawton, 2001). The Guerrero terrane has been described in southern Mexico as a composite terrane comprising island arc and back-arc basins, with or without oceanic crust, of Triassic to Early Cretaceous age (Campa and Coney, 1983; Centeno-García *et al.*, 1993, 2008; Bissig *et al.*, 2008; Mortensen *et al.*, 2008). This terrane was accreted to central Mexico during the Late Cretaceous (Centeno-García *et al.*, 1993; Busby *et al.* 2006) or during Late Cretaceous-early Tertiary Laramide Orogeny (Sedlock *et al.*, 1993; Dickinson and Lawton, 2001; Centeno-García *et al.*, 2008). The accretion produced low-grade metamorphism and some discrete folding (Campa and Coney, 1983; Centeno-García *et al.*, 1993).

METHODOLOGY AND ANALYTICAL TECHNIQUES

In this work we present the results of our geologic mapping of the Mesozoic of the Sierra de Zacatecas. Initial survey was made on synthetic stereopars made from a Landsat™ image (October 23rd, 2001) P029, R044 scale 1:150,000. The main structural features were recognized, and together with the geologic maps Zacatecas and Guadalupe, scale 1:50,000 (CETENAL, 1979a, 1979b), they were the bases for planning the survey. Detailed geologic mapping was made along many roads and creeks, with verification points each ~150 m or less when lithologic or structural changes were observed. We collected structural fault and foliation data throughout the stratigraphic section. Planes were measured using the right-hand rule. The notation used for planes is azimuth/dip/rake and for lines is plunge/trend (Marshak and Mitra, 1988). Fault planes show well developed striae, sometimes with precipitation of calcite and chlorite. Cataclastic bands or gouge developments are also common. The largest observed faults show displacements of less than a few meters; most of the faults show minor displacements. Kinematic indicators used were the ones described by Petit (1987). The analysis of foliation was carried out by separating the data by area.

Whereas the kinematic analysis was made accordingly

with the methodology proposed by Marret and Allmendinger (1990), fault data were separated depending on their stratigraphic position from bottom to top, the cross-cutting relationships (thrust faults are cut by normal faults), the quality of the data (well, moderately and poorly preserved), the rock type, and kinematic compatibility. The final results are shown by area.

Detrital zircons from one sample from the ZF (feldspathic greywacke) and one from LPVC (feldspathic wacke) were analyzed. The zircons were separated at the facilities of the Department of Geology, CICESE. The original rock samples, ~20 kg each one, were crushed and powdered. The -80 mesh fraction (≈ 200 μm) was selected and the zircons separated using a Wilfley table, a Frantz isodynamic separator, heavy liquids (methylene iodide) and nitric acid. The final separation was made by hand picking.

U-Pb geochronology of zircons was conducted by laser ablation multicollector inductively coupled plasma mass spectrometry (LA-MC-ICPMS) at the Arizona LaserChron Center. The analyses involved ablation of zircon with a New Wave/Lambda Physik DUV193 Excimer laser (operating at a wavelength of 193 nm) using a spot diameter of 35 microns. The collector configuration allows measurement of ^{204}Pb with an ion-counting channel, whereas ^{206}Pb, ^{207}Pb, ^{208}Pb, ^{232}Th and ^{238}U are measured simultaneously with Faraday detectors. All analyses were made in static mode with a laser beam diameter of 35 μm, operated with an output energy of 60 mJ at 23 kV and a pulse rate of 8 Hz. Data measurements, correction and error determination were performed as described by Gehrels *et al.* (2006). The results of the measurements for the ZF and LPVC are shown in Tables 1 and 2, respectively.

RESULTS

In this section we describe the stratigraphic sequences and structural data of the ZF and LPVC, which, together with the U-Pb dates of detrital zircons, will allow us to propose a tectonic scenario for both sequences.

Stratigraphy

Zacatecas Formation

As shown in Figures 2, and 3, the lowermost stratigraphic unit is the Zacatecas Formation (ZF), which crops out in the western part of the Sierra de Zacatecas (Figure 2). The ZF consists of phyllite, schist and slate showing significant variations in color, grain size and mineralogy. These differences are most likely related to changes in composition of the protolith rather than to changes in the degree of metamorphism. On a local scale, the ZF can be tightly folded. The original fabric can be obscured because of greenschists facies metamorphism and/or Tertiary hydrothermal alteration.

Primary sedimentary textures and composition of the ZF range from medium- to fine-grained sandstone and mudstone that contain a few conglomeratic layers and limestone lenses. Sandstones are quartz poor; feldspars and lithic fragments (plutonic, aphanitic and/or porphyritic volcanics) are rare to moderately abundant, and the matrix constitutes 26 to 70% of the rock. The shape of detrital components of the sandstones varies from subrounded to subangular. These rocks show a well-developed foliation defined by sericite. The thickness of individual strata is ≤50 cm, although the real thickness is difficult to define because the contact between sandstone and mudstone is commonly obliterated by foliation and/or weathering. The sedimentary succession of the ZF includes rare conglomeratic or conglomeratic sandstone layers that can be matrix or clast supported, with maximum thickness of ~40 m. The clasts are composed of quartzite and oxidized and/or silicified volcanic rocks(?). The clasts range in size from 1 cm up to ~5 cm, but occasionally can be as large as 30 cm in diameter. Limestone, sometimes folded, has also been identified in the ZF. Intercalated lava flows and probably also tuffs can be observed within the ZF. The presence of tuffs is not clear because the strong foliation and hydrothermal alteration obscure the primary structure and texture of the rock. However, we infer its presence from the existence of some broken euhedral to subhedral feldspar crystals in the sandstones. The lava flows are less foliated than the sedimentary rocks because of to their higher competence. The thickness of the lava flows can not be clearly defined because of the foliation, but it appears to be up to ~50 cm in some places. The lavas are porphyritic with argillitized plagioclase phenocrysts less than 1 mm in length. Chlorite is concentrated in the mafic minerals (clinopyroxene and olivine ?) and in the mafic phases(?) in the matrix. Hydrothermal epidote is also present. Pillow structures in lava flows, enclosing clastic sediments between the individual tubes are still present, indicating a submarine extrusion. Along the Arroyo El Bote, close to the type locality, the presence of a hydrothermal vent (see location in Figure 2) is suggested by horizons of brecciated quartz, lava blocks and sediment fragments in an aphanitic matrix (Figure 4). Plagioclase phenocrysts are also present in the matrix. Pervasive silicification and intense fracturing is observed around the vent, and some fractures are filled with hematite and magnetite. The intensity of fracturing and alteration decreases with increasing distance from the vent. Close to the vent there is a lava flow concordant to the sedimentary units of the ZF, which we interpret as related to the vent, suggesting that the volcanic activity took place during the deposition of the basin sediments. The vents are associated with the lava flows interbedded with the sediments. The lavas (Figure 4) are thin and some of them show pillow structures.

Las Pilas Volcanosedimentary Complex

The LPVC is exposed in the central and northern part of the SZ (Figure 2). Towards the dominant igneous LPVC is

Table 1. LA-ICPMS data of detrital zircons from the ZF, sample 88, Sierra de Zacatecas. Longitude: -102.62596ºW and Latitude: 22.78621ºN. (1) Sample identifier; (2) Isotope ratios corrected for common Pb using measured ^{204}Pb for correction. Individual errors are given as 1σ standard deviation.

Analysis (1)	^{206}Pb/^{204}Pb (2)	U (ppm)	U/Th	^{207}Pb*/^{235}U	±1σ (%)	^{206}Pb*/^{238}U	±1σ (%)	Error corr.	^{206}Pb*/^{238}U (Ma)	±1σ (Ma)	^{207}Pb*/^{235}U (Ma)	±1σ (Ma)	^{206}Pb*/^{207}Pb* (Ma)	±1σ (Ma)	Best age (Ma)	±1σ (Ma)
88-01	445	104	2.0	0.20585	20.6	0.02497	4.6	0.22	159.0	7.2	190.1	35.7	595.8	438.3	159.0	7.2
88-02	1377	550	3.7	0.16111	18.5	0.01977	8.3	0.45	126.2	10.3	151.7	26.0	570.5	361.4	126.2	10.3
88-03	1787	556	1.8	0.14479	4.8	0.02107	3.6	0.75	134.4	4.8	137.3	6.2	187.1	73.2	134.4	4.8
88-04	2280	710	0.9	0.17047	7.9	0.02516	3.3	0.41	160.2	5.2	159.8	11.7	154.9	169.5	160.2	5.2
88-05	611	96	2.4	0.34187	10.5	0.04577	5.8	0.56	288.5	16.5	298.6	27.2	378.3	196.9	288.5	16.5
88-06	999	171	0.9	0.35962	9.3	0.05250	2.9	0.31	329.9	9.3	311.9	24.9	180.0	206.0	329.9	9.3
88-07	6244	94	1.0	9.87342	5.7	0.40427	3.0	0.53	2188.7	55.4	2423.0	52.2	2626.2	79.9	2626.2	79.9
88-08	9358	362	3.9	1.81791U	4.3	0.17045	2.5	0.57	1014.6	23.2	1051.9	28.4	1130.3	70.9	1130.3	70.9
88-09	432	123	2.3	0.15533	14.7	0.02094	4.1	0.28	133.6	5.5	146.6	20.1	362.6	319.4	133.6	5.5
88-10	1799	323	1.6	0.29590	3.8	0.04072	2.7	0.70	257.3	6.7	263.2	8.8	316.1	61.9	257.3	6.7
88-11	4118	242	3.0	0.99257	8.6	0.11120	4.1	0.47	679.7	26.2	700.0	43.3	765.7	159.2	679.7	26.2
88-12	401	364	1.3	0.14532	16.6	0.02085	4.3	0.26	133.1	5.7	137.8	21.4	219.8	373.9	133.1	5.7
88-13	5000	226	3.0	1.64989	8.5	0.16256	5.9	0.69	971.0	53.2	989.5	53.8	1030.8	124.0	1030.8	124.0
88-13A	1064	442	1.0	0.13123	6.1	0.02029	3.2	0.52	129.5	4.1	125.2	7.2	43.9	124.2	129.5	4.1
88-14	2212	797	0.8	0.17092	3.0	0.02538	1.1	0.37	161.6	1.8	160.2	4.5	140.4	66.2	161.6	1.8
88-15	835	306	2.1	0.18009	5.9	0.02505	3.8	0.64	159.5	5.9	168.1	9.1	291.2	103.6	159.5	5.9
88-16	467	177	1.9	0.14891	13.2	0.02013	5.1	0.38	128.5	6.5	140.9	17.4	356.5	275.9	128.5	6.5
88-17	1653	875	1.2	0.16109	5.4	0.02370	2.7	0.50	151.0	4.0	151.7	7.6	162.0	109.5	151.0	4.0
88-18	459	142	1.2	0.15660	8.9	0.02044	3.8	0.43	130.4	4.9	147.7	12.2	435.2	179.2	130.4	4.9
88-19	778	288	1.7	0.13833	14.7	0.02096	3.8	0.26	133.7	5.0	131.6	18.1	92.2	337.2	133.7	5.0
88-20	747	202	1.6	0.16579	10.0	0.02645	4.3	0.43	168.3	7.1	155.8	14.4	-30.5	218.3	168.3	7.1
88-21	10722	864	10.2	0.58099	7.4	0.07425	3.9	0.53	461.7	17.3	465.1	27.5	481.9	138.8	461.7	17.3
88-22	4900	530	2.1	0.55339	3.6	0.07155	3.1	0.86	445.5	13.3	447.2	13.0	456.2	40.3	445.5	13.3
88-23	169	62	2.2	0.13521	20.0	0.01747	11.3	0.57	111.7	12.5	128.8	24.1	457.6	367.0	111.7	12.5
88-23A	2000	829	1.2	0.14157	7.9	0.02076	3.7	0.47	132.5	4.9	134.4	10.0	169.2	163.6	132.5	4.9
88-24	1461	433	1.4	0.14188	8.1	0.02185	5.9	0.72	139.3	8.1	134.7	10.2	54.1	133.6	139.3	8.1
88-25	2738	777	1.5	0.17035	6.9	0.02548	2.7	0.39	162.2	4.3	159.7	10.2	123.4	150.6	162.2	4.3
88-26	662	279	1.5	0.14746	7.9	0.02059	4.1	0.51	131.4	5.3	139.7	10.3	282.5	155.9	131.4	5.3
88-27	245	312	1.6	0.21564	25.7	0.02182	7.2	0.28	139.2	10.0	198.3	46.4	976.4	510.9	139.2	10.0
88-28	480	163	1.2	0.16909	8.6	0.02144	2.5	0.29	136.7	3.3	158.6	12.7	499.2	182.0	136.7	3.3
88-29	625	173	2.1	0.16712	12.5	0.02416	2.1	0.17	153.9	3.1	156.9	18.2	202.5	287.7	153.9	3.1
88-30	858	310	1.9	0.14655	6.4	0.02120	2.9	0.45	135.3	3.8	138.9	8.3	200.8	132.0	135.3	3.8
88-31	2483	897	14.9	0.16609	5.2	0.02366	4.4	0.83	150.8	6.5	156.0	7.6	236.6	67.3	150.8	6.5
88-32	282	96	2.4	0.12492	18.8	0.02082	6.8	0.36	132.8	8.9	119.5	21.2	-138.1	437.1	132.8	8.9
88-33	928	377	1.6	0.13863	5.9	0.02016	2.1	0.36	128.7	2.7	131.8	7.3	188.8	128.4	128.7	2.7
88-34	368	124	1.3	0.12569	12.8	0.02096	3.9	0.30	133.7	5.1	120.2	14.5	-139.0	303.0	133.7	5.1
88-35	302	96	1.8	0.13054	10.6	0.02046	4.7	0.44	130.5	6.1	124.6	12.5	12.5	229.5	130.5	6.1
88-36	2333	356	1.2	0.37690	6.2	0.05163	5.1	0.82	324.5	16.1	324.8	17.3	326.6	81.1	324.5	16.1
88-37	3635	2187	3.0	0.14443	5.2	0.02084	3.5	0.67	132.9	4.6	137.0	6.7	207.5	90.3	132.9	4.6
88-38	524	156	1.5	0.16901	10.6	0.02529	3.8	0.36	161.0	6.1	158.6	15.6	121.7	234.2	161.0	6.1
88-38A	24370	513	1.5	7.27949	6.3	0.39265	2.7	0.43	2135.1	48.7	2146.3	56.2	2157.0	99.4	2157.0	99.4
88-39	2753	1027	1.5	0.16883	5.8	0.02498	2.4	0.42	159.0	3.8	158.4	8.5	148.9	123.1	159.0	3.8
88-40	6386	348	2.6	1.79605	3.9	0.17790	1.9	0.49	1055.5	18.8	1044.0	25.6	1020.0	69.1	1020.0	69.1

All uncertainties are reported at the 1-sigma level, and include only measurement errors. Systematic errors would increase age uncertainties by 1-2%. U concentration and U/Th are calibrated relative to NIST SRM 610 and are accurate to ~20%. Common Pb correction is from ^{204}Pb, with composition interpreted from Stacey and Kramers (1975) and uncertainties of 1.0 for ^{206}Pb/ ^{204}Pb, 0.3 for ^{207}Pb/ ^{204}Pb, and 2.0 for ^{208}Pb/ ^{204}Pb. U/Pb and ^{206}Pb/ ^{207}Pb fractionation is calibrated relative to fragments of a large Sri Lanka zircon of 564 ± 4 Ma (2-sigma). U decay constants and composition as follows: ^{238}U = 9.8485 x 10^{-10}, ^{235}U = 1.55125 x 10^{-10}, ^{238}U/ ^{235}U = 137.88.

a transition characterized by an increase in the abundance of mafic lava flows, scarce tuffs, dikes, sills and laccolith-like bodies (Figure 3). Interlayered with the igneous rocks, there are a few feldspathic greywacke and wacke, mudstone, and limestone lenses; the sediment abundance increases upward the stratigraphic section.

Lava flows are the most abundant rock type in the LPVC. Based on the textural variations, we divided the extrusive sequence in massive and pillow-type, commonly foliated and/or deformed (Figures 2 and 3).

Massive flows are abundant in the SZ. Fracturing can be intense or absent, while foliation can vary from poorly

Table 2. LA-ICPMS data of detrital zircons from the LPVC, sample 40, Sierra de Zacatecas. Longitude: -102.50387ºW and Latitude: 22.82668ºN. (1) Sample identifier; (2) Isotope ratios corrected for common Pb using measured ^{204}Pb for correction. Individual errors are given in 1σ standard deviation.

Analysis (1)	^{206}Pb/^{204}Pb (2)	U (ppm)	U/Th	^{207}Pb*/^{235}U	±1σ (%)	^{206}Pb*/^{238}U	±1σ (%)	Error corr.	^{206}Pb*/^{238}U (Ma)	±1σ (Ma)	^{207}Pb*/^{235}U (Ma)	±1σ (Ma)	^{206}Pb*/^{207}Pb* (Ma)	±1σ (Ma)	Best age (Ma)	±1σ (Ma)
40-01	166	60	0.8	0.11752	25.2	0.02213	4.7	0.19	141.1	6.5	112.8	26.9	-449.0	660.5	141.1	6.5
40-02	322	93	0.6	0.16190	14.8	0.02420	4.7	0.32	154.1	7.2	152.4	20.9	124.7	331.2	154.1	7.2
40-03	326	117	1.5	0.12822	21.1	0.02156	9.8	0.46	137.5	13.3	122.5	24.3	-160.0	468.1	137.5	13.3
40-04	377	143	1.3	0.13297	9.8	0.02100	3.6	0.36	134.0	4.7	126.8	11.7	-6.9	221.6	134.0	4.7
40-05	452	160	1.0	0.12736	24.4	0.02260	3.7	0.15	144.1	5.2	121.7	28.0	-295.8	622.9	144.1	5.2
40-06	246	106	1.4	0.11859	12.8	0.01962	6.2	0.49	125.2	7.7	113.8	13.7	-119.6	275.9	125.2	7.7
40-07	255	118	1.5	0.12964	18.1	0.02024	5.5	0.30	129.1	7.0	123.8	21.1	21.8	416.2	129.1	7.0
40-08	305	125	0.9	0.19156	27.2	0.02120	6.6	0.24	135.2	8.9	178.0	44.4	792.0	562.6	135.2	8.9
40-09	294	31	0.9	0.32948	13.3	0.02124	6.5	0.49	135.5	8.7	289.2	33.6	1840.3	211.4	135.5	8.7
40-10	148	71	1.0	0.14084	48.5	0.02051	4.2	0.09	130.9	5.4	133.8	60.9	185.6	1190.4	130.9	5.4
40-11	340	127	0.9	0.14537	10.4	0.02337	5.3	0.51	148.9	7.9	137.8	13.4	-49.8	217.1	148.9	7.9
40-12	146	85	1.3	0.12179	17.4	0.02036	6.4	0.37	129.9	8.2	116.7	19.2	-145.9	403.2	129.9	8.2
40-13	586	363	1.8	0.15859	21.9	0.02116	7.8	0.36	135.0	10.4	149.5	30.5	386.3	464.3	135.0	10.4
40-14	476	480	1.4	0.15152	15.2	0.02212	4.6	0.30	141.0	6.5	143.3	20.4	179.9	340.1	141.0	6.5
40-15	491	150	1.4	0.13846	11.2	0.02177	6.4	0.57	138.8	8.8	131.7	13.8	4.5	222.0	138.8	8.8
40-17	409	76	1.1	0.13194	19.5	0.02238	2.3	0.12	142.7	3.3	125.8	23.0	-181.6	486.3	142.7	3.3
40-18	191	96	0.7	0.12862	19.2	0.02209	8.2	0.43	140.8	11.4	122.9	22.2	-212.6	437.7	140.8	11.4
40-19	322	128	1.2	0.12406	9.3	0.02003	3.7	0.40	127.8	4.7	118.7	10.4	-60.0	206.8	127.8	4.7
40-20	233	110	1.1	0.12179	16.3	0.02026	9.0	0.55	129.3	11.5	116.7	18.0	-133.2	337.7	129.3	11.5
40-20A	350	189	0.9	0.12993	22.2	0.02050	5.3	0.24	130.8	6.9	124.0	25.9	-3.8	523.9	130.8	6.9

All uncertainties are reported at the 1-sigma level, and include only measurement errors. Systematic errors would increase age uncertainties by 1-2%. U concentration and U/Th are calibrated relative to NIST SRM 610 and are accurate to ~20%. Common Pb correction is from ^{204}Pb, with composition interpreted from Stacey and Kramers (1975) and uncertainties of 1.0 for ^{206}Pb/^{204}Pb, 0.3 for ^{207}Pb/^{204}Pb, and 2.0 for ^{208}Pb/^{204}Pb. U/Pb and ^{206}Pb/^{207}Pb fractionation is calibrated relative to fragments of a large Sri Lanka zircon of 564 ± 4 Ma (2-sigma). U decay constants and composition as follows: ^{238}U = 9.8485 x 10^{-10}, ^{235}U = 1.55125 x 10^{-10}, ^{238}U/^{235}U = 137.88.

to moderately developed. The massive flows, when foliated, always show a well developed foliation defined by chlorite. Foliated flows are found next to dioritic intrusions, which suggests that the competent dioritic bodies acted as stress barriers during the deformation phase. The deformed flows exhibit poorly to moderately developed foliation, brecciation and/or intense fracturing that makes difficult to recognize any internal structure. The pillowed lavas, by contrast, have a well developed pillow structure, lava tubes and sometimes fine grained sediments between the pillows. The size of the pillows varies from ~30 cm to ~1 m. Over the lava tubes it is sometimes possible to distinguish striae presumably formed by the overriding flow. No specific stratigraphic distribution is observed for each extrusive igneous type. However, towards the top of the sequence massive flows covered by pillowed lavas are conspicuous.

The mineralogy of the flows consists of ≤1%, quartz and 0 to 30% plagioclase phenocrysts (An$_{20}$ to An$_{45}$), clinopyroxene phenocrysts varying from 0 to 34%. Olivine, when present, can be as much as 3%. Plagioclase and clinopyroxene can be also found as aggregates forming a glomerophyric texture. Matrix varies from microcrystalline to cryptocrystalline. Lava flows have intense hydrothermal and/or deuteric alteration, which promoted the formation of sericite, calcite, epidote and chlorite.

In some places, the boundaries between lava flows and intrusive bodies are not clear and both kinds of units show the same textural relationships in thin section. These observations together with the crystal abundance suggest that some magma could have been emplaced in a melt-impregnated regime involving subsurface crystallization that promoted the formation of dikes and sills as proposed in the model of Reid (2003).

Most intrusive bodies are dikes and sills and may evolve to laccolith-like plutons (Figure 2, sections A-A' and B-B'). The laccolithic intrusions are almost elliptical in plan view. Their size is less than 2 km in diameter. The contacts between the intrusive and sedimentary rocks are normally sharp but, when the intrusives are in contact with the lava flows, the boundaries are not easily recognized. The intrusions can be highly fractured, faulted (brittle faulting) and/or hydrothermally altered. Essential minerals in laccoliths, dikes and sills are similar both in abundance and composition with respect to lava flows: quartz (≤1%), plagioclase from An$_{20}$ to An$_{45}$ and abundances that varies from 25 to 50%; clinopyroxene varies from 3 to 25%. The olivine, when present, is less than 3%. Mafic minerals are altered to chlorite, whereas plagioclase is altered to calcite and sericite. The textures are phaneritic, porphyritic, traquitoid and poikilitic, in this order of decreasing abundance. In the last one the plagioclase is the oikocryst.
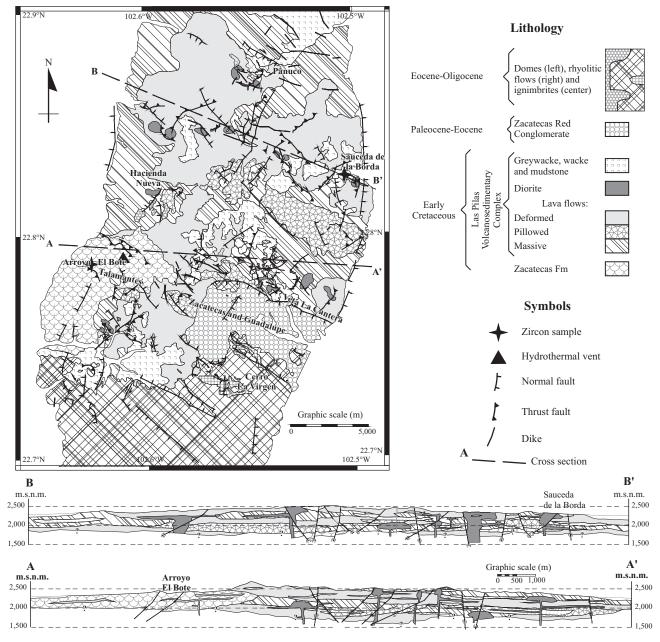
Figure 2. Geologic map of the Mesozoic sequence of the Sierra de Zacatecas. For clarity of the map the urban boundaries are not shown. The names of towns are in bold, whereas the ones of topographic features not. A-A' and B-B' are cross sections orientated ~E-W across northern and southern Mesozoic sequence of the SZ. Notice the different scales in map and cross sections.

Apparently, dikes and sills have developed from the laccoliths. The thickness of the dikes can reach 10 m and sometimes the dikes change into sills following the bedding planes. The sills can have a thickness near to 2 m and extend for about ~1.5 km. It seems that the dikes were emplaced as melt-impregnated bodies in a shallow environment, more or less contemporaneous with the extrusion of the lava flows. Locally, the dikes can be abundant, but thin (~1 m in thickness). These dikes are close to laccolithic intrusions from which they probably derived.

A sequence made up by greywacke, wacke, mudstone, and scarce sandstone, tuff and limestone is interlayered and

covering the volcano-plutonic suite of the LPVC. Near the boundary between the ZF and LPVC, these sediments show a well developed foliation. Moving upward in the stratigraphic column, foliation becomes weaker and is indistinguishable from bedding at the top. Detritic sedimentary rocks are matrix rich (>20%). Detrital components include quartz, either mono- or polycrystalline, and plagioclase; the abundance of lithic fragments vary considerably. The individual layers of sediments are < 50 cm in thickness, and show a rhythmic interbedding of greywacke, wacke and mudstone. Upsection, the amount of sediments increase in abundance, and near the top of the sequence the thickness

can be >50 m. The interlayering of the different detrital sediments defines a flysch-like deposit. Limestone occurs as lenses less than 4 m thick. The limestone outcrops, which are mostly interlayered with the deformed or pillowed lava flows, are not always associated with the detrital record. Owing to the recrystallization and weathering, it was not possible to identify the internal characteristics of the limestone. The sedimentary assemblages are interlayered with the lava flows and are cut by the intrusive suite in sharp contact.

An interpretation of the internal distribution of the LPVC and ZF is shown in the cross-sections A-A' and B-B' (Figure 2). As will be discussed later, the distribution of igneous rocks and sediments suggests the existence of a volcanic field in an island arc or in its back-arc basin.
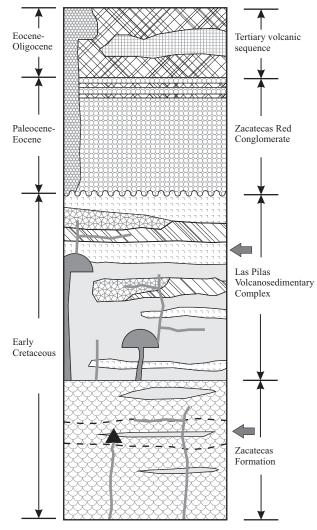

Figure 3. Stratigraphic column of the Sierra de Zacatecas. The legend is the same as in Figure 2. Age of the sequence is based on the range intervals obtained by U-Pb analysis of detrital zircons by LA-ICPMS. Gray arrows indicate the stratigraphic location where the detrital zircons were separated. Dashed lines show the approximate location of Unit B of Ranson *et al.*, (1982), sometimes called La Pimienta Formation (Monod and Calvet, 1992) of previously reported Triassic age. Black triangle shows the approximate location of the interpreted hydrothermal vent.

Cenozoic sequence

The Mesozoic stratigraphic sequence of the SZ is unconformably overlain by the Zacatecas Red Conglomerate (ZRC) (Figure 3). The age of the ZRC has been previously reported as Paleocene (Ponce y Clark, 1988). The conglomerate is supported by a sandy matrix and has a distinctive red color. The ZRC is well to moderately consolidated; their clasts are subangular to subrounded varying in size from 2 mm to about 5 cm, occasionally they can be up to 30 cm in diameter. Clasts fragments are made of quartzite, phyllite, schist, diorite and mafic rocks. Although no granitic bodies have been recognized in the SZ, a few layers of the ZRC are granitoid rich. Most of the clasts originated from the Mesozoic rocks described before. Strata are irregular in shape, structureless, massive, and in channels, belonging to fluvial or alluvial sediments deposited in a fault-bounded basin. The ZRC crop out only in the Zacatecas and Guadalupe urban areas (Figure 2), filling a roughly E-W trending basin bounded to the north by the south dipping Veta La Cantera normal fault and to the south by several small faults dipping north. The upper part of the ZRC is interbedded with thin layers, less than 50-cm thick, of air-fall tuffs. The Eocene-Oligocene geologic record of the SZ consists of air-fall and ash-flow tuffs, volcanic breccias, rhyolitic flows and a few and thin conglomeratic red beds interlayered with the volcanics. Rhyolitic to dacitic dikes cut the entire sequence. Most of the Tertiary volcanic outcrops are located south of Zacatecas and Guadalupe cities in the Cerro La Virgen (Figure 2).

U-Pb ages of detrital zircons

For this study, we separate detrital zircons for U-Pb dating from a sandstone layer of the ZF (Figures 2 and 3) close to the place were Bruckhardt (1906) described fossils of Late Triassic age. The results of U-Pb *in situ* dating analyses of the 43 detrital zircons obtained from the sample 88 are shown in Table 1 and in Figure 5b. The detrital zircons from the ZF gave two main picks at 132 and 160 Ma, followed by minor Paleozoic and Precambrian clusters which involve about 30% of the data (Figure 5b). The ages obtained for the ZF clearly indicate a maximum depositional age of this sequence in the Early Cretaceous (Hauterivian), which is significantly younger than the formerly proposed Late Triassic age.

From the LPVC we obtained a sample, close to the Sauceda de la Borda town (Figure 2), from a feldspathic wacke to separate detrital zircons. The U-Pb ages obtained from the LA-ICPMS measurements of 20 grains (Table 2) cluster at ~132 and ~160 Ma (Figure 5a). As in the previous case, these ages suggest a maximum depositional age of the Early Cretaceous (Hauterivian). The wacke strata come from La Borda Formation, inferred to be Cretaceous by Miriam Yta (*in* Centeno-García and Silva-Romo, 1997).

Figure 4. Interpreted hydrothermal vent intruding the ZF. Notice the brecciation and alteration. Fracturing and hydrothermal alteration are intense around the vent, and decreases away from it. Vertical black arrows show some of the brecciated lava blocks. Horizontal white arrows show the sediments.

Structural geology

The upper part of the Mesozoic stratigraphic section shows a change in deformation style when compared with the lower part. The ZF has mostly experienced ductile deformation; whereas the LPVC experienced brittle deformation. In the ZF, the foliation obliterates most of the striae, resulting in only limited fault data.

The intensity of foliation within the ZF varies with the mechanical strength of the rock; the fine grained sedimentary layers are more intensely foliated then the coarse grained rocks or lava flows. Locally, the layers of the ZF can be tightly folded, although no large folds have been recognized. At microscopic scale, the ZF has slaty cleavage, "beards" and a few sigma porphyroclasts; the foliation is defined mainly by sericite.

In the LPVC the foliation development decreases towards the upper part of the stratigraphic section. The sedimentary layers of the lower part can have pencil-like structure, which is absent in the upper strata. The cross-cutting fault relationships indicate that thrust faults are older than the normal ones.

The foliation data are shown together with the kinematic analysis of thrust faulting in areas of kinematic compatibility (Figure 6). In the area 1, fault trending is mainly directed towards N 40–70º W, S 20–40º E and S 60–70º E, in that order of abundance; other structures are perpendicular to these orientations (Figure 6, area 1, "a"). For this area, the shortening axes show a wide dispersion in the stereogram (Figure 6, area 1, "b"), with a significant grouping in the NE and SW quadrants. Their average compression axis (σ1) is 03º/041º. The poles to foliation are located at the center-right of the stereogram, showing a barely lineal trend directed to the NE-SW (Figure 6, area 1, "c"). In this area, the normal faults have three dominant orientations at

N 40–50º W, N 70–80º E and N 20–30ºW, in that order of abundance (Figure 7, area 1, "a"). Their extension axes show some dispersion in the stereogram, with a concentration in the NE and SW quadrants. Their average extension axis (σ3) is located at 01º/025º (Figure 7, Area 1, "b"). In the area 1, the σ1 orientation for thrust faults is approximately perpendicular to the trend of the main thrust and normal faults; and to the orientation of the foliation planes.

In the area 2, thrust faulting has three preferred orientations: S 70–80º E, S 20–30º E and N 10–20º W, with similar abundance (Figure 6, area 2, "a"). Their shortening axes are mainly located in the NE quadrant, with the average compression axis (σ1) at 06º/091º. In the same area, the normal faults are mostly directed towards N 20–40º W, N 50–60º W and N 80–90º W (Figure 7, area 2, "a"); they have less dispersion than the thrust faults. Their extension axes are located dominantly in the NE and SW quadrants with the average extension axis (σ3) located at 15º/045º (Figure 7, area 2, "b"). The normal and thrust faults show some parallelism; however, thrust faulting is more randomly oriented than normal faults. The shortening and extension axes of both kinds of faulting are largely located in the NE and SW quadrants. The paleostress axes for both types of faulting are located in the NE quadrant, as in area 1 (Figures 6 and 7), suggesting that normal faulting developed by extension
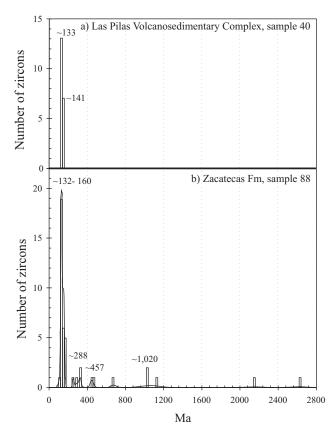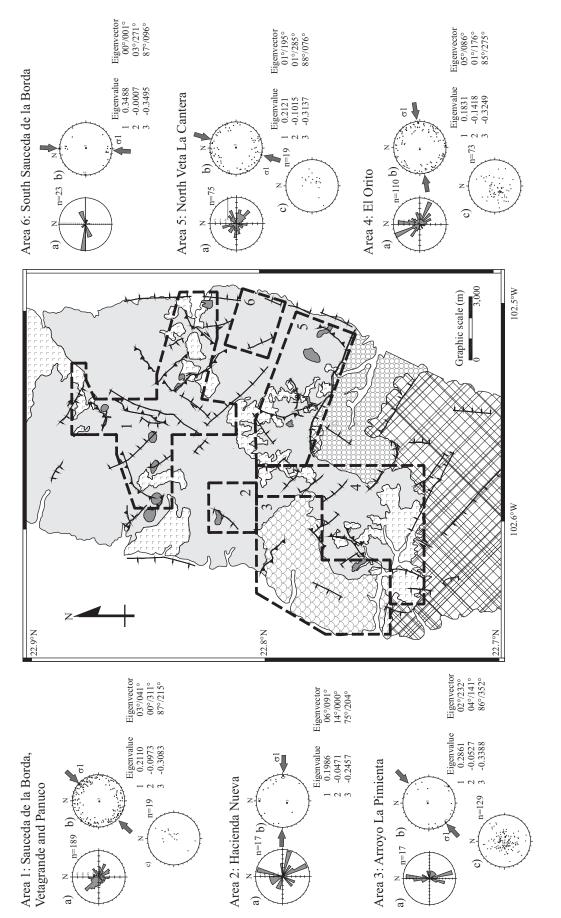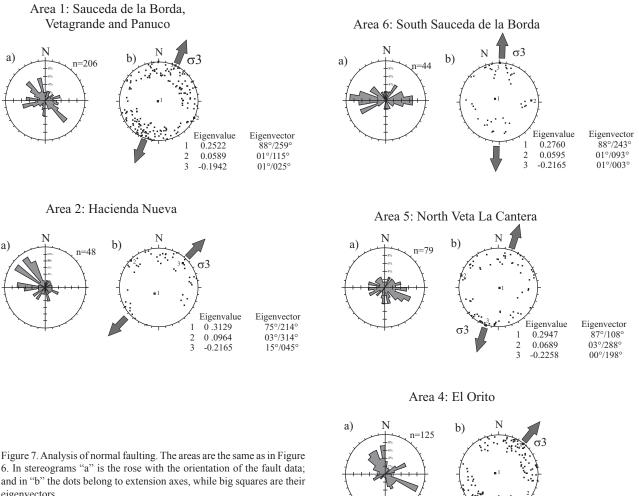

Figure 5. Histograms of U-Pb ages obatined for detrital zircons of (a) Las Pilas Volcanosedimentary Complex (20 data) and (b) Zacatecas Fm. (43 data). Black bold line separates the samples. Ages in Ma.

Area 6: South Sauceda de la Borda

a)   b)

	Eigenvalue	Eigenvector
1	0.3488	00°/001°
2	-0.0007	03°/271°
3	-0.3495	87°/096°

Area 5: North Veta La Cantera

a)   b)   c)

	Eigenvalue	Eigenvector
1	0.2121	01°/195°
2	-0.1015	01°/285°
3	-0.3137	88°/076°

Area 4: El Orito

a)   b)   c)

	Eigenvalue	Eigenvector
1	0.1831	05°/086°
2	-0.1418	01°/176°
3	-0.3249	85°/275°

Area 1: Sauceda de la Borda, Vetagrande and Panuco

a)   b)   c)

	Eigenvalue	Eigenvector
1	0.2110	03°/041°
2	-0.0973	00°/311°
3	-0.3083	87°/215°

Area 2: Hacienda Nueva

a)   b)

	Eigenvalue	Eigenvector
1	0.1986	06°/091°
2	-0.0471	14°/000°
3	-0.2457	75°/204°

Area 3: Arroyo La Pimienta

a)   b)   c)

	Eigenvalue	Eigenvector
1	0.2861	02°/232°
2	-0.0527	04°/141°
3	-0.3388	86°/352°

Figure 6. Analysis of thrust faulting and foliation of the Mesozoic sequence of the Sierra de Zacatecas. The legend is the same as in Figure 2, except for the lava flows that for clarity have been merged in one unit. n=number of data. Roses of fault data are unidirectional. Stereograms are in lower hemisphere, equal area. In the geologic map areas bounded by heavy dashed lines and pointed out with a dash-dot line are: 1) Sauceda de la Borda, Vetagrande and Pánuco, 2) Hacienda Nueva, 3) Arroyo La Pimienta, 4) El Orito, 5) North Veta La Cantera and 6) South Sauceda de la Borda. In each area "a" is the rose with the orientation of fault data, dots in stereograms "b" are shortening axes, while the big squares are the location of the paleostresses axes. Dots in stereograms "c" are poles to foliation planes.

Area 1: Sauceda de la Borda,
Vetagrande and Panuco

Area 6: South Sauceda de la Borda

	Eigenvalue	Eigenvector
1	0.2760	88°/243°
2	0.0595	01°/093°
3	-0.2165	01°/003°

	Eigenvalue	Eigenvector
1	0.2522	88°/259°
2	0.0589	01°/115°
3	-0.1942	01°/025°

Area 2: Hacienda Nueva

Area 5: North Veta La Cantera

	Eigenvalue	Eigenvector
1	0.3129	75°/214°
2	0.0964	03°/314°
3	-0.2165	15°/045°

	Eigenvalue	Eigenvector
1	0.2947	87°/108°
2	0.0689	03°/288°
3	-0.2258	00°/198°

Area 4: El Orito

Figure 7. Analysis of normal faulting. The areas are the same as in Figure 6. In stereograms "a" is the rose with the orientation of the fault data; and in "b" the dots belong to extension axes, while big squares are their eigenvectors.

	Eigenvalue	Eigenvector
1	0.2899	83°/285°
2	0.0776	07°/129°
3	-0.2124	03°/039°

due to residual stresses after the compressive stage.

The thrust faults in area 3 are mainly directed towards N 0–10º E and S 10–20º E (Figure 6, area 3, "a"). Resulting shortening axes are chiefly located in the NE and SW quadrants with their compression axis (σ1) located at 02º/232º (Figure 6, area 3, "b"). In this area, the poles to foliation are dispersed throughout the central part of the stereogram, although a minor NNW-SSE and NE-SW trends can be observed (Figure 6, area 3, "c"). The NNW-SSE trend is perpendicular to the σ1 orientation, which suggests a genetic relationship.

In El Orito area (Figure 6, area 4), the trend of thrust faults is N 20–30º W, S 60–70º E, and N 0–10º E, in this order of abundance (Figure 6, area 4, "a"). The shortening axes show some dispersion but can be grouped in the NE and SW quadrants. The average compression axis (σ1) is located at 05º/086º (Figure 6, area 4, "b"). The poles to foliation are located at the center-left of the stereogram (Figure 6, area 4, "c"), with a trend roughly perpendicular to the orientation of σ1. The normal faults trends are mostly S 60–70º

E, N 0–10º W, N 20–50º W and N 60–70º E, in this order of abundance (Figure 7, area 4, "a"). Their extension axes are mostly grouped in the NE and SW quadrants, with the average at 03º/039º (Figure 7, area 4, "b"). The thrust and normal faults trends are mainly located in the NW and SE quadrants; as well as their shortening and extension axes, respectively.

In the area 5, thrust faults are mainly oriented towards the NW and SE quadrants, with a few data in the other ones (Figure 6, area 5, "a"). Their shortening axes are largely located in the NE and SW quadrants with an average compression axis (σ1) located at 01º/195º (Figure 6, area 5, "b"). The foliation poles show certain grouping at center-right of the stereogram (Figure 6, area 5, "c"). Normal faulting is mostly directed towards S 40–70º E (Figure 7, area 5, "a"). Their extension axes tend to group in the NE and SW quadrants with σ3 located at 00º/198º (Figure 7, area 5, "b"). In area 5, the thrust and normal faults trends are mostly parallel, as well as their shortening and extension axes. Some normal faults are parallel to the orientation of the foliation.

In area 6, the thrust faults are oriented to N 80–90º E and N 70–80º E (Figure 6, area 6, "a"). Their shortening axes are located in the NNE and SSW positions in the stereogram, so that their average compression axis is 00º/001º (Figure 6, area 6, "b"). The normal faults mainly trend N 70–90º W and N 60–90º E, in this order of abundance (Figure 7, area 6, "a"). Their extension axes are largely grouped at the northern and southern parts of the stereogram with an average extension axis located at 01º/003º (Figure 7, area 6, "b").

From the paleostress analysis of each region shown in Figures 6 and 7, the resulting principal paleostress directions were plotted in Figures 8a and 8b. For normal and thrust faulting, the average σ1 and σ3 are directed towards the SW and NE, respectively. For the analysis of the displacement and sense of slip we show the different rake, dip and sense of slip for all the faults of the SZ (Figure 8c). The lack of specific trends or groups of data for any region may be due to the small displacement shown by the faults, the lithologic changes and/or the subtle changes in the paleostress direc-

tion. Figure 8c shows that the normal faults have dip angles larger than 30º, whereas only a few thrust faults have angles lower than 30º, with rakes over 60º. Fault displacements and dips show a wide dispersion that could be related to local mechanical discontinuities produced by the interlayering of sediments in the lava flows, or the presence of the more rigid intrusive bodies. The mechanical effect can also be related to the thickness and extent of massive and pillowed lava flows. Another hypothesis for the dispersion of the fault data is that, since the basement in the Zacatecas Volcanic Field is unknown, the mapped stratigraphic sequence can be repeated downward, in such a way that the interlayering of ductile and brittle layers could promote the dispersion of fault data.

DISCUSSION

Based on field relationships, structural analysis and U-Pb dating of zircons, the more likely explanation for

Figure 8. Average of σ1 (a) (1st) and σ3 (b) (2nd) for each area of Figures 6 and 7. Contour intervals each 2σ. Large squares are the paleostress average for all sigmas. c) Relationships dip *vs.* rake and the sense of slip of the faults (Angelier, 1984).

the geologic relationships between the Zacatecas Fm. and the Las Pilas Volcanosedimentary Complex is that they belong to the same stratigraphic unit. This study support earlier interpretations on the origin of the metamorphic and "green rocks" of the Sierra de Zacatecas, which suggested that they belong to the same stratigraphic entity (Gutiérrez-Amador, 1908; McGehee, 1976; Ranson *et al.*, 1982). Our age dating analysis shows that detrital zircons of the ZF and LPVC have similar ages at *ca.* 132 and 160 Ma. The maximum depositional age of the detrital zircons indicate that the Mesozoic sequence of the SZ is of Early Cretaceous (Hauterivian) age.

The protoliths of the ZF are sandstone, mudstone, limestone, a few conglomerate and lava flows. Lava flows and some tuffaceous horizons interlayered with fine grained sediments are present towards the top of the ZF. Sandstone contains broken euhedral to subhedral feldspar crystals, together with subrounded feldspar crystals and volcanic lithics, which suggest a volcanic source close to the place where the ZF and LPVC were deposited and emplaced. The ZF outcrops are located only in the central-western part of the SZ. The limited distribution of the lava flows and volcaniclastics, as well as the lithologic assemblage, suggest a shallow marine environment and a marked volcanic influence, as previously proposed by Gutiérrez-Amador (1908) and Monod and Calvet (1992). Previous workers have interpreted that the ZF is a submarine fan formed in a deep marine environment later translated and deformed during Jurassic time (McGehee, 1976; Sedlock *et al.*, 1993; Centeno-García and Silva-Romo, 1997; Bartolini *et al.*, 2001). Barboza-Gudino *et al.*, (1999) suggested that this fan was deposited close to the present-day location. An alternative environment for the deposition of the ZF and the emplacement and deposition of the LPVC sequences is in either an immature arc as in Guanajuato (Lapierre *et al.*, 1992; Ortiz-Hernández *et al.*, 1992) or in the vecinity of Zacatecas city (Mortensen *et al.*, 2008), or in an ocean floor environment (Centeno-García and Silva-Romo, 1997; Centeno-García *et al.*, 2008). In that kind of basins, subsidence could have led to deposition of alternating layers of sediments and volcaniclastic. As the volcanic complex evolved, lava flows became the dominant rock type. The distribution of the igneous and sedimentary rocks schematically represented in Figure 2 support the presence of a volcanic field of Early Cretaceous age in this part of Mexico. The basin could be related to the Late Jurassic-Early Cretaceous island arc of the Guerrero terrane (Campa and Coney, 1983; Sedlock *et al.*, 1993; Centeno-García and Silva-Romo, 1997; Dickinson and Lawton, 2001). The nearest area where the Guerrero terrane crops out is in Guanajuato (Figure 1), where several workers have described lithologic sequences interpreted to be part of a Late Jurassic-Early Cretaceous island arc (Lapierre *et al.*, 1992; Tardy *et al.*, 1992, 1994; Freydier *et al.*, 1996, 2000; Ortiz-Hernández *et al.*, 2000). An alternative scenario is the allochtonous origin of the ZF as proposed by other authors. During Middle Jurassic

time, a considerable translation occurred associated to the Mojave-Sonora Megashear (Sedlock *et al.*, 1993; Jones *et al.*, 1995; Bartolini *et al.*, 2001) and processes of accretion, subduction and/or collision (Sedlock *et al.*, 1993; Centeno-García and Silva-Romo, 1997) prior to the emplacement of the LPVC. However, deformation of the ZF is characterized by greenschists facies metamorphism and faults with small displacements. Based on these observations, Ranson *et al.*, (1982) and Monod and Calvet (1992) suggested the presence of major thrust in the ZF with small displacements. As expected, folding and the development of foliation in the ZF are related to the composition and mechanical strength of the layers. The ductile deformation of the ZF could be related to a shallow environment heated by the intrusions of magmatic bodies such as dikes, sills and associated volcanism in an island arc environment as shown in the Figure 2. Towards the east, the brittle deformation observed in places within the LPVC, could be related to emplacement forces of the igneous bodies and to the stronger mechanical resistance of the lava flows and subvolcanic diorites with respect to the sedimentary layers.

The results of the paleostress analysis (Figure 8) indicate a NE-SW oriented trend for compression and extension, parallel to the stress orientation during the Laramide Orogeny of Late Cretaceous-Early Tertiary (Monod and Calvet, 1992; Sedlock *et al.*, 1993; Centeno-García and Silva-Romo, 1997; Bartolini *et al.*, 2001). The amount of shortening during the Laramide Orogeny has been estimated in ~90 km or 40% in a section of the frontal part of the chain in San Luis Potosí (Suter, 1987), whereas other authors suggests ~150 km or 30% of shortening in other areas (Sedlock *et al.*, 1993). Whatever the distance of transport or the amount of shortening, most of the deformation has been accommodated in the ZF in a ductile mode, and by dominantly brittle deformation in the LPVC. A tentative hypothesis is that these differences, together with the location of the laccoliths, could have promoted the dispersion of the data shown in the Figures 6, 7 and 8c.

The LPVC has been correlated to the origin and evolution of the Guerrero terrane or superterrane, which is well documented in southern Mexico and has been interpreted as an island arc of Late Jurassic-Early Cretaceous time (Campa and Coney, 1983; Delgado-Argote et al., 1992; Sedlock *et al.*, 1993; Centeno-García and Silva-Romo, 1997; Dickinson and Lawton, 2001; Talavera-Mendoza *et al.*, 2007).

The lithologic and geochronologic data presented in this paper indicate that the Mesozoic sequence of the Sierra de Zacatecas can be correlated with the Guerrero terrane. The most probable tectonic setting where the Mesozoic Zacatecas Volcanic Field could have been developed is presented in Figure 9. The sedimentary supply, as shown by the detrital zircon age distribution, indicates Precambrian and Mesozoic sources for the ZF. As the volcanic field evolved and the back arc developed, a change in the sedimentary supply occurred, as observed in the detrital zircon ages for the LPVC. In this scenario, an intra-arc or back-arc basin

with sedimentary input from the arc and from the continent is a suitable model for the development of the Mesozoic sequence of the SZ. This model allows the correlation of the Mesozoic Zacatecas Volcanic Field with the island arc and back-arc basin of Late Jurassic-Early Cretaceous that outcrops in Guanajuato.

CONCLUSIONS

In the Arroyo El Bote and in Sauceda de la Borda areas in the Sierra de Zacatecas, the contact between the Zacatecas Fm. and the overlying Las Pilas Volcanosedimentary

Complex is interpreted to be gradual since no visual hiatus or major tectonic overthrusting has been recognized. The stratigraphic continuity of both formations is supported by similar peak ages of detrital zircons in two distinct sedimentary horizons (*ca.* 132 and 160 Ma) that point to a similar provenance. The occurrence of both Paleozoic and Proterozoic zircon grains in the lower ZF indicates a continental provenance of the sediments. With respect to the paleogeographic setting; the zircons were most likely derived from the North American Craton and an island arc. The relationships between sedimentary and igneous rocks suggest the presence of a volcanic arc providing sediments to an intra-arc or back-arc setting, similar to other

Figure 9. a) Schematic scenario for the Early Cretaceous formation and emplacement of the Mesozoic stratigraphic sequence of the Sierra de Zacatecas, also shown the position of North American craton and the island arc of the Guerrero terrane. The age intervals show the possible sources for the detrital zircons. b) Cross section show the initial stage (Late Jurassic?) of the Mesozoic Zacatecas Volcanic Field with a continental sedimentary supply; c) and a later stage (Early Cretaceous) of the island arc and back-arc basin of the Guerrero terrane and the possible location of the deposit and emplacement of the Zacatecas Formation (ZF) and Las Pilas Volcanosedimentary Complex (LPVC). Not to scale.

sequences of the Guerrero terrane. In combination with the North American cratonic provenance of the zircons, the depositional facies can be assumed to be part of an active continental margin setting.

The maximum depositional age for the sequence, indicated by the ages of youngest detrital zircons (*ca.* 132 Ma), is a relevant information for the reconstruction of the Mesozoic terranes of Mexico. Despite the amount of zircons analyzed, the data included in this work are the first isotopic ages published for the Sierra de Zacatecas; this Early Cretaceous age (Hauterivian) is the first isotopic time marker for the sequence and is significantly younger than most previously suggested ages.

The deformation style of the Mesozoic SZ shows a NE-SW trend for both normal and thrust faulting. The SZ has ductile deformation at the bottom, and the stratigraphic section changes upward to a brittle style. All the poles of the foliation planes are close to the vertical, suggesting folds with large amplitude. On the basis of crosscutting relationships of the faults we propose that the compressive stage was followed by extension after the Laramide orogeny. The stress applied produced small displacements on the faults, perhaps due to the brittle-ductile coupling of the Mesozoic of the SZ and the small amount of shortening that occurred during the Laramide orogeny. All stresses applied during the Mesozoic evolution of the SZ were directed towards the northeast.

ACKNOWLEDGMENTS

REFERENCES

Angelier, J, 1984, Tectonic Analysis of Fault Slip Data Sets: Journal of Geophysical Research, 89(B7), 5835-5848.

Aranda-Gómez, J.J., Henry, C.D., Luhr, J.F., 2000, Evolución tectonomagmática postpaleocénica de la Sierra Madre Occidental y de la porción meridional de la provincia tectónica de Cuencas y Sierras, México: Boletín de la Sociedad Geológica Mexicana, 53, 59-71.

Barboza-Gudino, J.R., Tristán-González, M., Torres-Hernández, J.R., 1999, Tectonic setting of pre-Oxfordian units from central and northeastern Mexico: A review, *in* Bartolini, C., Wilson, J.L., Lawton, T.F. (eds.), Mesozoic Sedimentary and Tectonic History of North-Central Mexico: Boulder, Colorado, Geological Society of America, Special Paper 340, 197-210.

Bartolini, C., Lang, H., Cantú-Chapa, A., Barboza-Gudiño, R., 2001, The Triassic Zacatecas Formation in central Mexico: Paleotectonic, paleogeographic, and paleobiogeographic implications, *in* Bartolini, C., Buffler, R.T., Cantú-Chapa, A. (eds.), The western Gulf of Mexico Basin: Tectonics, sedimentary basins, and petroleum systems: American Association of Petroleum Geologists (AAPG) Memoir, 75, 295-315.

Bissig, T., Mortensen, J.K., Tosdal, R.M., Hall, B.V., 2008, The rhyolite-hosted volcanogenic massive sulfide disctrict of Cuale, Guerrero Terrane, west-central Mexico: Silver-rich, base metal mineralization emplazed in a shallow marine continental margin setting: Economic Geology, 103, 141-159.

Burckhardt, C., 1906, Sobre el descubrimiento del Triásico marino en Zacatecas: Boletín de la Sociedad Geológica Mexicana, 2, 43-45.

Busby, C., Fackler-Adams, B., Mattinson, J., Deoreo, S., 2006, View of an intact oceanic arc, from surficial to mesozonal levels: Cretaceous Alisitos arc, Baja California: Journal of Volcanology and Geothermal Research, 149, 1-46.

Campa, F., Coney, P., 1983, Tectono-stratigraphic terranes and mineral resource distribution in Mexico: Canadian Journal of Earth Sciences, 20, 1040-1051.

Centeno-García, E., Silva-Romo, G., 1997, Petrogenesis and tectonic evolution of central Mexico during Triassic-Jurassic time: Revista Mexicana de Ciencias Geológicas, 4(2), 244-260.

Centeno-García, E., Ruíz, J., Coney, P.J., Patchett, P.J., Ortega-Gutiérrez, F., 1993, Guerrero terrane of Mexico: Its role in the Southern Cordillera from new geochemical data: Geology, 21, 419-422.

Centeno-García, E., Guerrero-Suastegui, M., Talavera-Mendoza, O., 2008, The Guerrero composite terrane: Collision and subsequent rifting in a supra-subduction zone, *in* Draut, A., Clift, P.D., Scholl, D.W. (eds.), Formation and Applications of the Sedimentary Record in Arc Collision zones: Geological Society of America, Special Paper 436, 279-308.

Comisión de Estudios del Territorio Nacional (CETENAL), 1979a, Carta geológica Zacatecas (F13B58), escala 1:50,000: Secretaría de Programación y Presupuesto, Comisión de Estudios del Territorio Nacional, 1 mapa.

Comisión de Estudios del Territorio Nacional (CETENAL), 1979b, Carta geológica Guadalupe (F13B68), escala 1:50,000: Secretaría de Programación y Presupuesto, Comisión de Estudios del Territorio Nacional, 1 mapa.

De Cserna, Z., 1976, Geology of the Fresnillo area, Zacatecas, Mexico: Geological Society of America Bulletin, 87, 1191-1199.

Delgado-Argote, L.A., López-Martínez, M., York, D., Hall, C.M., 1992, Geologic framework and geochronology of ultramafic complexes in southern Mexico: Canadian Journal of Earth Sciences, 29, 1590-1604.

Dickinson, W.R., Lawton, T.F., 2001, Carboniferous to Cretaceous assembly and fragmentation of Mexico: Geological Society of America

Bulletin, 113(9), 1142-1160.

Freydier, C., Martinez-R., J., Lapierre, H., Tardy, M., Coulon, C., 1996, The Early Cretaceous Arperos oceanic basin (western Mexico): Geochemical evidence for an aseismic ridge formed near an spreading center: Tectonophysics, 259, 343-367.

Freydier, C., Lapierre, H., Briqueu, L., Tardy, M., Coulon, C., Martínez-Reyes, J., 1997, Volcaniclastic sequences with continental affinities within the Late Jurassic-Early Cretaceous Guerrero intra-oceanic arc terrane (western Mexico): The Journal of Geology, 105, 483-502.

Freydier, C., Lapierre, H., Ruiz, J., Tardy, M., Martínez-R., J., Coulon, C., 2000, The Early Cretaceous Arperos basin: an oceanic domain dividing the Guerrero arc from nuclear Mexico evidenced by the geochemistry of lavas and sediments: Journal of South American Earth Sciences, 13, 325-336.

Gastil, R.G. Miller, R., Anderson, P., Croecker, J., Campbell, M., Buch, P., Lothringer, C., Leier-Engelhardt, P., DeLattre, M., Hoobs, J., Roldán-Quintana, J., 1991, The relation between the Paleozoic strata on the opposite sides of the Gulf of California, *in* Pérez-Segura, E., Jacques-Ayala, C. (eds.), Studies of Sonoran Geology: Geological Society of America, Special Paper 254, 7-18.

Gastil, G., Rector, G., Hazelton, G., Al-Riyami, R., Hanes, J., Farrar, E., Böhnel, H., Ortega-Rivera, A., García-Guzmán, J., 1999, Late Cretaceous pillow basalt, siliceous tuff and calc-turbidite near Porohui, northern Sinaloa, Mexico, *in* Bartolini, C., Wilson, J.L., Lawton, T.F. (eds.), Mesozoic Sedimentary and Tectonic History of North-Central Mexico: Boulder, Colorado, Geological Society of America, Special Paper 340,145-150.

Gehrels, G., Valencia, V., Pullen, A., 2006, Detrital Zircon Geochronology by Laser Ablation Multicollector ICPMS at the Arizona LaserChron Center, *in* Olszewski, T. (ed.), Geochronology: Emerging Opportunities: Paleontology Society Papers, 12, 67-76.

Goldhammer, R.K., 1999, Mesozoic sequence stratigraphy and paleogreographic evolution of northeast Mexico, *in* Bartolini, C., Wilson, J.L., Lawton, T.F. (eds.), Mesozoic Sedimentary and Tectonic History of North-Central Mexico: Geological Society of America, Special Paper 340, 1-58.

Gutiérrez-Amador, M., 1908, Las capas Cárnicas de Zacatecas: Boletín de la Sociedad Geológica Mexicana, 4, 29-35..

Jones, N.W., McKee, J.W., Anderson, T.H., Silver, L.T., 1995, Jurassic volcanic rocks in northeastern Mexico: A possible remnant of a Cordilleran magmatic arc, *in* Jacques-Ayala, C., González-León., C., Roldán-Quinatana, J. (eds.), Studies on the Mesozoic of Sonora and Adjacent Areas: Boulder, Colorado, Geological Society of America, Special Paper 301, 179- 190.

Lapierre, H., Ortiz, L.E., Abouchami, W., Monod, O., Coulon, C., Zimmermann, J.L., 1992, A crustal section of an intra-oceanic island arc: The Late-Jurassic-Early Cretaceous Guanajuato magmatic sequence, central Mexico: Earth and Planetary Science Letters, 108, 61-77.

Marshak S., Mitra, G., 1988, Basic methods of structural geology, Part I: Elementary techniques: New Jersey, Englewood Cliffs, Prentice Hall, 446 pp.

Marret, R. and Allmendinger, R.W., 1990, Kinematic analysis of fault-slip data: Journal of Structural Geology, 12, 973-986.

McGehee, R.V., 1976, Las rocas metamórficas del Arroyo La Pimienta, Zacatecas, Zac.: Boletín de la Sociedad Geológica Mexicana, 37(1), 1-10.

Monod, O., Calvet. P., 1992, Structural and stratigraphic re-interpretation of the Triassic units near Zacatecas (Zac.), Central Mexico: Evidence of a Laramide nappe pile: Zentralblatt für Geologie und Paläontologie, Teil I, 6, 1533-1544.

Mortensen, J.K., Hall, B.V., Bissig, T., Friedman, R.M., Danielson, T., Oliver, J., Rhys, D.A., Ross, K.V., Gabites, J.E., 2008, Age and paleotectonic setting of volcanogenic massive sulfide deposits in the Guerrero Terrane of central Mexico: Constraints from U-Pb age and Pb isotope studies: Economic Geology, 103, 117-140.

Ortega-Gutiérrez, F., Prieto-Vélez, R., Zúñiga, Y., Flores, S., 1979, Una secuencia volcano-plutónica-sedimentaria Cretácica en el norte

de Sinaloa; ¿Un complejo ofiolítico?: Universidad Nacional Autónoma de México, Revista del Instituto de Geología, 3(1), 1-8.

Ortiz-Hernández, L.E., Chiodi, M., Lapierre, H., Monod, O., Calvet, P., 1992, El arco intraoceánico alóctono (Cretácico Inferior) de Guanajuato –Características petrográficas, geoquímicas, estructurales e isotópicas del complejo filoniano y de las lavas basálticas asociadas; implicaciones geodinámicas: Universidad Nacional Autónoma de México, Revista del Instituto de Geología, 9(2), 126-145

Ortiz-Hernández, L.E., Acevedo-Sandoval, O.A., Flores-Castro, K., 2003, Early Cretaceous intraplate seamounts from Guanajuato, central Mexico: geochemical and mineralogical data: Revista Mexicana de Ciencias Geológicas, 20(1), 27-40.

Palmer, A.R., 1983, The Decade of North American Geology, 1983 Geologic Time Scale: Geology, 11(9), 503-504.

Petit, J.P., 1987, Criteria for the sense of movement on fault surfaces in brittle rocks: Journal of Structural Geology, 9, 597-608

Ponce, B.F., Clark, K.F., 1988, The Zacatecas mining district: A Tertiary caldera complex associated with precious and base metal mineralization: Economic Geology, 83, 1668- 1682

Ranson, W.A., Fernández, L.A., Simmons; Jr., W.B., Enciso-de la Vega, S., 1982, Petrology of the metamorphic rocks of Zacatecas, Zac., Mexico: Boletin de la Sociedad Geológica Mexicana, 43(1), 37-59.

Reid, M.R., 2003, Timescales of magma transfer and storage in the crust, *in* Rudnick, R.L. (ed.), The Crust: Oxford, UK, Elsevier, Treatise on Geochemistry, Holland, H.D., Turekian, K.K. (executive eds.), v. 3, 167-193..

Sedlock, R.L., Ortega-Gutiérrez, F., Speed, R.C., 1993, Tectonostratigraphic terranes and tectonic evolution of Mexico: Geological Society of America, Special Paper 278, 153 pp.

Silva-Romo, G., Arellano-Gil, J., Mendoza-Rosales, C., Nieto-Obregón, J., 2000, A submarine fan in the Mesa Central, Mexico: Journal of South American Earth Sciences, 13, 429-442.

Suter, M., 1987, Structural traverse across the Sierra Madre Oriental fold-thrust belt in east-central Mexico: Geological Society of America Bulletin, 95, 249-264.

Talavera-Mendoza, O., Ruiz, J., Gehrels, G.E., Valencia, V.A., Centeno-García, E., 2007, Detrital zircon U/Pb geochronology of southern Guerrero and western Mixteca arc successions (southern Mexico): New insights for the tectonic evolution of southwestern North America during the late Mesozoic: Geological Society of America Bulletin, 119(9), 1052-1065.

Tardy, M., Maury, R., 1973, Sobre la presencia de elementos de origen volcánico en las areniscas de los flyschs de edad cretácica superior de los estados de Coahuila y de Zacatecas-México: Boletín de la Sociedad Geológica Mexicana, 34(1-2), 5-12.

Tardy, M., Lapierre, H., Bourdier, J.L., Coulon, C., Ortiz-Hernández, L.E., Yta, M., 1992, Intraoceanic setting of the western Mexico Guerrero terrane –implications for the Pacific-Thetys geodynamic relationships during the Cretaceous: Universidad Nacional Autónoma de México, Revista del Instituto de Geología, 10(2), 118-128.

Tardy, M., Lapierre, H., Freydier, C., Coulon, C., Gill, J.B., Mercier de Lepinay, B., Beck, C., Martínez-R., J., Talavera-M., O., Ortiz-H, E., Stein, G., Bourdier, J.L., Yta, M., 1994, The Guerrero suspect terrane (western Mexico) and coeval arc terranes (the Greater Antilles and the Western Coordillera of Colombia): a late Mesozoic intra-oceanic arc accreted to cratonal America during the Cretaceous: Tectonophysics, 230, 49-73.

Yta, M., Moreno-Tovar, R., Cardona-Patiño, F., Córdoba-Méndez, D. A., 2003, Contribución a la definición de superposición de eventos metalogénicos en el yacimiento de Francisco I. Madero: Revista Mexicana de Ciencias Geológicas, 20(2), 124-132.